NETWORKS AND HETEROGENEOUS MEDIA
©American Institute of Mathematical Sciences
Volume **2**, Number **1**, March **2007**

Website: http://aimSciences.org

pp. **99–125**

DERIVATION AND ANALYSIS OF A FLUID-DYNAMICAL MODEL IN THIN AND LONG ELASTIC VESSELS

Debora Amadori

Dip. di Matematica Pura e Applicata
Università degli Studi dell'Aquila
Via Vetoio, 67010 Coppito (AQ), Italy

Stefania Ferrari and Luca Formaggia

MOX, Dip. di Matematica "F. Brioschi"
Politecnico di Milano
P.zza Leonardo da Vinci 33, 20133 Milan, Italy

(Communicated by Roberto Natalini)

Abstract. Starting from the three-dimensional Newtonian and incompressible Navier-Stokes equations in a compliant straight vessel, we derive a reduced one-dimensional model by an averaging procedure which takes into consideration the elastic properties of the wall structure. In particular, we neglect terms of the first order with respect to the ratio between the vessel radius and length. Furthermore, we consider that the viscous effects are negligible with respect to the propagative phenomena. The result is a one-dimensional nonlinear hyperbolic system of two equations in one space dimension, which describes the mean longitudinal velocity of the flow and the radial wall displacement. The modelling technique here applied to straight cylindrical vessels may be generalized to account for curvature and torsion. An analysis of well posedness is presented which demonstrates, under reasonable hypotheses, the global in time existence of regular solutions.

1. **Introduction.** The use of reduced models to study the fluid-structure interaction in compliant vessels is rather well established. Typical applications range from the haemodynamics of large arteries to the investigation of hammer effects in hydraulic networks. These models are quite accurate in the description of the wave propagation phenomena typical of this type of problems and are much cheaper in terms of computational cost compared to a full three-dimensional model.

An increased interest in these models in the context of haemodynamic applications has been driven by the "geometrical multiscale approach" for simulating the mutual interaction between local and systemic dynamics (see [10],[12],[13]). In this frame, reduced models play the role of representing the global behavior of the circulatory system or large parts of it, which interact with local descriptions made by means of more sophisticated models. One-dimensional models are of interest here because of their capability of accurately representing pulse waves in large arteries (see [24], [22]).

2000 *Mathematics Subject Classification.* Primary: 76Z05, 35L50; Secondary: 74F10, 35Q30.
Key words and phrases. Physiological flows, fluid-structure interaction, hyperbolic equations.

Simplifying assumptions are usually necessary for their derivation. In particular, it is assumed that the flow is mainly in the axial direction and that the effects of the viscosity are negligible with respect to the propagative effects under study. Indeed the viscous terms are either completely neglected, as in [22], or accounted for by a source term, as in [23] and [4]. Here, we justify the neglect of the viscous term by comparing its contribution against the other terms in the equations, for the typical values of the parameter in the target application. Moreover we suppose that the profile of the axial component of the velocity is such that the non-linear advective term in the momentum equation can be suitably treated. Under these hypotheses we are able to derive a system of just two equations that describe the evolution of mean flux and pressure. With respect to the derivation of a similar model, we have avoided to make any assumption that could impede the generalization of the model to curved vessels. Therefore, even if the results here presented are specialized for straight vessels, the derivation can be generalized to a different metric. Work is indeed ongoing in this direction and this extension will be the subject of a forthcoming paper.

The derivation of the model follows closely that of [4], the main difference being the treatment of the equations for the wall displacement.

We mention that in [5] a different one-dimensional model for compliant vessels is advocated, which does not require any closure assumption on the longitudinal velocity profile. The authors show that the model is accurate to the second order with respect to the ratio between the vessel radius length scales. However, this model requires us to solve an additional equation and its complexity reduces its applicability in practice.

The role of longitudinal displacements of the vessel wall has been recently pointed out in [7]. This work shows their small relative importance for haemodynamic applications, which are the main concern of the present work. Therefore we have chosen to describe the vessel wall in terms of a linear elastic and axi-symmetric structure which allows only radial displacements. Differently from previous works we will not use a shell type representation of the structure as we preferred to derive the law governing the structure dynamics directly from the Navier equation, through some simplifying assumptions. By our asymptotic analysis we finally obtain an algebraic law linking the pressure to the measure of the vessel section, which is constant on each cross-section as in [4]. The resulting expression is indeed similar to that obtained for membrane shells, with a correction term that accounts for moderately thick walls. This algebraic law can be used as a closing relation for our one dimensional model.

The way of reducing the three-dimensional Navier-Stokes system and of handling the boundary conditions proposed in the present article, has been inspired by the derivation of the equations for shallow water flow introduced in [16] and later refined in [8] and in [9]. In particular we consider the dynamic boundary conditions prescribing the equilibrium of the stresses at the fluid-structure interface and the kinematic conditions which guarantee the continuity of the radial velocity at the fluid-structure interface. On the other hand, in [23] and [4] the authors force the longitudinal and the circumferential components of the velocity to vanish at the fluid-structure interface and they impose continuity of the radial velocity.

The more common one-dimensional models present in the literature, and our model as well, are given by hyperbolic systems of two differential equations in one space dimension. In [4] a rather complete mathematical analysis is carried out in the

space-time half-plane. In particular they analyze the blow-up of regular solutions due to the non linear effects in the case that the system is homogeneous with no source term. They find that, the typical vessel length of an artery is much shorter than the space required for a discontinuity to develop, the wave propagation in the arterial system may be considered of regular type.

In this paper we present a more general well posedness analysis and prove the global in time existence of regular solutions on a bounded spatial domain, in the case of constant coefficients and no source term. The results is applicable to a wide range of boundary conditions. In particular, we have considered either pressure or velocity prescribed at one end while at the other end we account for "resistive type" boundary conditions. The latter, which includes a non-reflecting boundary condition as a particular case, models the resistance to the flow caused by the peripheral circulatory system. The non-reflecting condition is obtained when the resistance parameter is set to zero. The analysis is applicable to a wide class of one-dimensional models, including the most commonly adopted in the biomedical literature. Finally, we have then assessed our result with a numerical test.

The outline of this paper is as follows. In the Section 1 we introduce the three-dimensional fluid-structure interaction model we are moving from and the rescaling of the system needed for the successive derivations. In the Section 2 we derive the one-dimensional system by averaging the rescaled model. In the Section 3, we provide a complete mathematical analysis. In the Section 4 we provide some numerical experiments in order to validate our new model and compare it with the model previously proposed in [23]. Some conclusions are drawn in Section 5 and some details on the geometrical framework we are dealing with are collected in the Appendix at the end of the paper.

2. **The 3D fluid-structure-interaction model.**

In this section we detail the fluid and the vessel wall dynamics in cylindrical coordinates in their respective space-time domains. We describe the wall dynamics through a linear elastic and isotropic stress-strain law as in [14]. We also consider only radial displacements. Furthermore, we will assume that the shear component of the Cauchy stresses at the wall are negligible once the equations are written in the natural coordinate frame of the vessel wall.

The imposition of the continuity of the radial velocity and of the stresses at the fluid-structure interface completes the setting of the 3D fluid-structure interaction model.

Finally, by introducing a suitable rescaling of the whole model we approximate the equations to the first order with respect to the ratio between the vessel radius and length and derive a first-order approximate expression for the pressure of the fluid.

2.1. **The fluid-dynamics.**

Let $L > 0$ be the total length of an axi-symmetric vessel with circular cross-section, let $T > 0$ be the total evolution time and let

$$\eta : [0, T] \times [0, L] \to \mathbb{R}^+, \qquad \eta_0 : [0, L] \to \mathbb{R}^+$$

be the radial distance of the fluid-wall interface from the centerline (see Fig. 1), during the motion and in the reference configuration, respectively. We are here assuming that the vessel wall allows only radial displacements. The space domain we are dealing with may be described in cylindrical coordinates, using the notation

$$x^1 = r, \quad x^2 = \theta, \quad x^3 = z,$$

where z is aligned along the vessel axis, and is assumed fixed. We refer to [2] for a reminder of vector analysis in the cylindrical coordinate system.

At any $t \in [0, T]$ the fluid domain is given by

$$\mathcal{U} = \{(r, \theta, z) \in [0, \eta(t, z)) \times [0, 2\pi) \times (0, L)\}.$$

Its boundary is split into three different parts: the inlet $\mathcal{L}_{in}$, the outlet $\mathcal{L}_{out}$ and the vessel wall interface $\mathcal{S}$ (see Fig. 1)[1]. We have, for $t \in [0, T]$

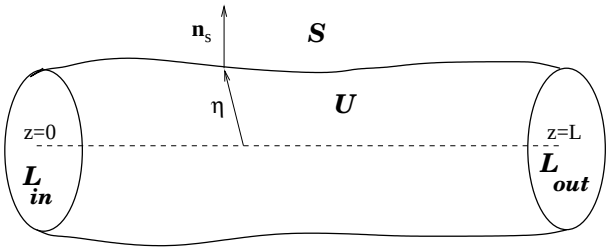

FIGURE 1. The time-dependent axi-symmetric domain $\mathcal{U}$ and its boundary at a given time t

$$\mathcal{L}_{in} = \{(r, \theta, 0) : (r, \theta) \in [0, \eta(t, 0)) \times [0, 2\pi)\},$$
$$\mathcal{L}_{out} = \{(r, \theta, L) : (r, \theta) \in [0, \eta(t, L)) \times [0, 2\pi)\}$$

while

$$\mathcal{S} = \{(\eta(t, z), \theta, z) : (\theta, z) \in [0, 2\pi) \times (0, L)\}, \quad t \in [0, T]. \tag{1}$$

We will indicate the outward radial normal to $\mathcal{S}$ by $\boldsymbol{n}_{\mathcal{S}}$. It may be readily verified that its coordinates are given in physical components by

$$\boldsymbol{n}_{\mathcal{S}} = c_s \left(1, 0, -\frac{\partial \eta}{\partial z}\right) \quad \text{with } c_s = \left[1 + \left(\frac{\partial \eta}{\partial z}\right)^2\right]^{-1/2}. \tag{2}$$

From now on we will adopt the summation convention and, whenever not otherwise indicated, repeated indices i, j, k, l run from 1 to 3. Furthermore, we will indicate the physical components of a tensor B in cylindrical coordinates either as $B(ij)$ or, alternatively, as B_{rr}, $B_{r\theta}$ etc.

2.2. **The Navier-Stokes equations.** The physical components of the rate of deformation tensor D in (physical) cylindrical coordinates are

$$D_{rr} = \frac{\partial u_r}{\partial r}, \quad D_{\theta\theta} = \frac{1}{r}\frac{\partial u_\theta}{\partial \theta} + \frac{u_r}{r}, \quad D_{zz} = \frac{\partial u_z}{\partial z}, \quad D_{rz} = \frac{1}{2}\left(\frac{\partial u_r}{\partial z} + \frac{\partial u_z}{\partial r}\right),$$
$$D_{r\theta} = \frac{1}{2}\left(r\frac{\partial}{\partial r}\left(\frac{u_\theta}{r}\right) + \frac{1}{r}\frac{\partial u_r}{\partial \theta}\right), \quad D_{z\theta} = \frac{1}{2}\left(\frac{1}{r}\frac{\partial u_z}{\partial \theta} + \frac{\partial u_\theta}{\partial z}\right)$$

while the components of the Cauchy stress tensor T_N for a Newtonian fluid are given by

$$T_N(ij) = -P\delta^{ij} + \hat{\sigma}(ij),$$

[1] In haemodynamic applications the terms proximal and distal are usually referred to as inlet and outlet, respectively

being P the pressure, δ^{ij} the Kronecker symbol and $\hat{\sigma}(ij) = 2\hat{\mu}D(ij)$, where $\hat{\mu}$ is the viscosity of the fluid. It is a common practice to divide the momentum equation by the constant density. We will therefore indicate

$$\frac{T_N(ij)}{\varrho} = -p\delta^{ij} + \sigma(ij)$$

where $\sigma(ij) = 2\mu D(ij)$, while μ is here the kinematic viscosity and p is the pressure scaled by the fluid density. Finally, the Navier-Stokes equations in cylindrical coordinates may be written as

$$\begin{cases} \dfrac{\partial}{\partial r}(ru_r) + \dfrac{\partial u_\theta}{\partial \theta} + \dfrac{\partial}{\partial z}(ru_z) = 0\,, \\ \dfrac{\partial u_r}{\partial t} + \dfrac{1}{r}\dfrac{\partial\left(ru_r^2\right)}{\partial r} + \dfrac{1}{r}\dfrac{\partial\left(u_r u_\theta\right)}{\partial \theta} + \dfrac{\partial(u_r u_z)}{\partial z} - \dfrac{1}{r}u_\theta^2 = \\ \qquad -\dfrac{\partial p}{\partial r} + \dfrac{1}{r}\dfrac{\partial\left(r\sigma_{rr}\right)}{\partial r} + \dfrac{1}{r}\dfrac{\partial \sigma_{r\theta}}{\partial \theta} + \dfrac{\partial \sigma_{rz}}{\partial z} - \dfrac{\sigma_{\theta\theta}}{r}\,, \\ \dfrac{\partial u_\theta}{\partial t} + \dfrac{\partial(u_r u_\theta)}{\partial r} + \dfrac{1}{r}\dfrac{\partial(u_\theta^2)}{\partial \theta} + \dfrac{\partial(u_\theta u_z)}{\partial z} + \dfrac{2}{r}u_\theta u_r = \\ \qquad -\dfrac{1}{r}\dfrac{\partial p}{\partial \theta} + \dfrac{\partial \sigma_{r\theta}}{\partial r} + \dfrac{1}{r}\dfrac{\partial \sigma_{\theta\theta}}{\partial \theta} + \dfrac{\partial \sigma_{\theta z}}{\partial z} + \dfrac{2}{r}\sigma_{r\theta}\,, \\ \dfrac{\partial u_z}{\partial t} + \dfrac{1}{r}\dfrac{\partial(ru_r u_z)}{\partial r} + \dfrac{1}{r}\dfrac{\partial(u_z u_\theta)}{\partial \theta} + \dfrac{1}{r}\dfrac{\partial\left(ru_z^2\right)}{\partial z} = \\ \qquad -\dfrac{\partial p}{\partial z} + \dfrac{1}{r}\dfrac{\partial(r\sigma_{rz})}{\partial r} + \dfrac{1}{r}\dfrac{\partial \sigma_{z\theta}}{\partial \theta} + \dfrac{1}{r}\dfrac{\partial\left(r\sigma_{zz}\right)}{\partial z}\,. \end{cases} \tag{3}$$

2.3. **The dynamics of the vessel wall.** We will consider here the equations necessary to account for the wall compliance. Following the route usually taken to derive reduced models we will assume that the wall inertia is negligible, that is the wall is instantaneously in equilibrium. However, differently from [4], we here derive the reduced model directly from the basic equations of continuum mechanics, under suitable hypothesis. The configuration at time t of the vessel wall is given by:

$$\mathcal{W} = \{(r,\theta,z) : (\theta,z) \in [0,2\pi) \times (0,L), r \in [\eta(t,z), \eta(t,z) + k(t,z)]\}$$

where $k = k(t,z) > 0$ indicates the thickness of the wall. The inner part of the vessel wall coincides with the fluid-structure interface $\mathcal{S}$ introduced in (1) (see Figure 2). More precisely $\mathcal{W}_{|r=\eta} = \mathcal{S}$. The current and the reference position of a point of the wall is given respectively by:

$$\boldsymbol{w} : (0,T) \times \mathcal{W} \to \mathbb{R}^3, \quad \boldsymbol{w}_0 : \mathcal{W} \to \mathbb{R}^3$$

where $\boldsymbol{w}$ depends on the dynamics of the wall, while $\boldsymbol{w}_0$ is a known function. For a complete description of function $\boldsymbol{w}$ see (66) in the Appendix. On the wall it is also possible to identify a different coordinate system, (s,θ,l), aligned with the current configuration. Its definition is detailed in the Appendix as well. Since we are considering only radial displacements, we may write

$$w_\theta = w_{0\theta}, \quad w_z = w_{0z}.$$

Furthermore, we have the following identities, for $(t,\theta,z) \in (0,T) \times (0,2\pi] \times (0,L)$:

$$\eta(t,z) = w_r(t,\eta(t,z),\theta,z), \qquad \eta_0(z) = w_{0r}(\eta_0(z),\theta,z)\,.$$

Let ψ^i be the 1-contravariant displacement vector given by

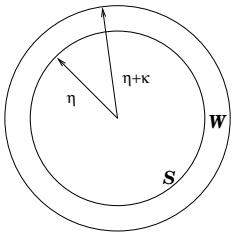

FIGURE 2. The time-dependent axi-symmetric domain $\mathcal{W}$

$$\psi^1 = w_r - w_{0r}, \quad \psi^2 = w_\theta - w_{0\theta} = 0, \quad \psi^3 = w_z - w_{0z} = 0.$$

The general formulation of the infinitesimal strain tensor in 2-covariant form (see [14]) is

$$e_{ij} = \frac{1}{2}\left(\psi_{i,|j} + \psi_{j,|i}\right) = \frac{1}{2}\left(\frac{\partial \psi_i}{\partial x^j} + \frac{\partial \psi_j}{\partial x^i}\right) - \Gamma^l_{ij}\psi_l$$

where Γ^l_{ij} are the Christoffel symbols connected to the orthogonal metric (68). The familiar linear elastic relation that provides the Cauchy stress tensor is given by

$$T_{ij} = 2Ge_{ij} + \lambda e_{kk} g_{ij}$$

and, in physical components,

$$T(ij) = 2Ge(ij) + \lambda e_{kk}\delta_{ij} \tag{4}$$

where G and λ are, in general, functions of z. It is worth recalling the usual relationships

$$G = \frac{E}{2(1+\xi)}, \qquad \lambda = \frac{\xi E}{(1-2\xi)(1+\xi)} \tag{5}$$

where $E \geq 0$ is the Young modulus and $\xi \in (0, 1/2)$ the Poisson ratio. We will consider the following hypotheses:

1. The thickness of the vessel is uniform, that is $k(t,z) = k_0$ and is small in comparison with the radius of the vessel.
2. As a consequence of the previous assumption we consider that $e_{\theta\theta}$ is constant across the thickness of the vessel wall. In particular we will set $e_{\theta\theta} = \frac{\eta - \eta_0}{\eta}$.
3. The Cauchy stress tensor is aligned with the local reference frame $\boldsymbol{t}$, $\boldsymbol{n}$, $\boldsymbol{b}$ (see the Appendix). That is, in this reference frame shears are negligible (see [15]). This assumption derives from the fact that the fibers that form the structural part of the wall of a blood vessel are approximately aligned with the local frame and show little resistance to bending. As a consequence, the Cauchy stress tensor in the local reference frame, here indicated by $\mathcal{T}$, is assumed to be diagonal.
4. We neglect the inertial effects in the wall structure, that is the wall structure is always in static equilibrium.
5. We finally assume that the pressure external to the vessel is zero. This is not a restrictive hypothesis since the isotropic contribution of the external pressure may be added a-posteriori.

Exploiting (4) and recalling the usual relationship between the traces $\mathcal{T}_{kk} = (2G + \lambda)e_{kk}$ and assumption 3, we can express the components of the (diagonal)

elastic stress tensor $\mathcal{T}$ in the local reference frame $\mathbf{t}$, $\mathbf{n}$, $\mathbf{b}$ as

$$\begin{cases} \mathcal{T}_{\theta\theta}(\eta) = 2G\frac{\eta-\eta_0}{\eta} + \frac{\xi}{1+\xi}(\mathcal{T}_{ss}(\eta) + \mathcal{T}_{\theta\theta}(\eta) + \mathcal{T}_{ll}(\eta)) \\ \mathcal{T}_{ll}(\eta) = \frac{\xi}{1+\xi}(\mathcal{T}_{ss}(\eta) + \mathcal{T}_{\theta\theta}(\eta) + \mathcal{T}_{ll}(\eta)), \end{cases} \tag{6}$$

on the fluid structure interface $r = \eta$. In order to close the system we evaluate $\mathcal{T}_{ss}(\eta)$ by solving the equation of static equilibrium along the direction $\mathbf{n}$. By using the symbols s, θ and l to denote the physical components, as described in the Appendix, the equilibrium in the s direction gives

$$0 = [\mathbf{div}(\mathcal{T})]_s = \frac{1}{h_\theta h_l}\frac{\partial}{\partial s}\left(\frac{h_\theta h_l}{h_s}\mathcal{T}_{ss}\right) + \frac{1}{h_s}\Gamma^s_{ss}\mathcal{T}_{ss} + \frac{h_s}{h_\theta^2}\Gamma^s_{\theta\theta}\mathcal{T}_{\theta\theta} + \frac{h_s}{h_l^2}\Gamma^s_{ll}\mathcal{T}_{ll}. \tag{7}$$

In our case

$$h_s = 1, \quad h_\theta = r = \eta + s\cos\psi, \quad h_l = 1 + s\chi,$$

and

$$\Gamma^s_{ss} = 0 \quad \Gamma^s_{\theta\theta} = -r\cos\psi \quad \Gamma^s_{ll} = -\chi(1+s\chi),$$

where the quantities $\cos\psi$ and χ depend on the geometry and are defined in (67). Therefore, (7) gives

$$\frac{1}{r}\left[\frac{\partial}{\partial s}\left(r(1+s\chi)\mathcal{T}_{ss}\right) - \cos\psi(1+s\chi)\mathcal{T}_{\theta\theta}\right] - \chi\mathcal{T}_{ll} = 0. \tag{8}$$

Integrating (8) over the wall thickness $0 \le s \le k_0$ and recalling that a zero external pressure implies that $\mathcal{T}_{ss} = 0$ for $s = k_0$, we obtain a relation between $\mathcal{T}_{ss}(\eta)$, $\mathcal{T}_{\theta\theta}(\eta)$ and $\mathcal{T}_{ll}(\eta)$. Taking relations (6) into account, it is possible to obtain an explicit form for $\mathcal{T}_{ss}(\eta)$, $\mathcal{T}_{\theta\theta}(\eta)$ and $\mathcal{T}_{ll}(\eta)$. However, we will postpone this calculation after an a-dimensionalization procedure which points out the terms which are proportional to the ratio between the scales of the vessel radius and the length, which are supposed to be small and then negligible by our asymptotic analysis.

It is possible to obtain the Cauchy stress tensor T with respect to the global (cylindrical) reference frame. To this purpose it is sufficient to perform a rotation around the θ-axis, that is

$$T = R\mathcal{T}R^T,$$

where the rotation matrix R is given by

$$R = \begin{bmatrix} n_r & 0 & -n_z \\ 0 & 1 & 0 \\ n_z & 0 & n_r \end{bmatrix}. \tag{9}$$

Here n_r and n_z are the radial and longitudinal components of the outward normal to the fluid-structure interface $\boldsymbol{n}_\mathcal{S}$ introduced in (2).

2.4. **Boundary conditions at the fluid-structure interface.** At the fluid-structure interface we have the continuity of the normal stresses, that is we may write

$$T_N \cdot \boldsymbol{n}_\mathcal{S} - T \cdot \boldsymbol{n}_\mathcal{S} = 0. \tag{10}$$

Thanks to (9) and the definition of the normal vector we have

$$T \cdot \boldsymbol{n}_\mathcal{S} = R\mathcal{T}R^T \cdot \boldsymbol{n}_\mathcal{S} = \begin{bmatrix} n_r\mathcal{T}_{ss} \\ 0 \\ n_z\mathcal{T}_{ss} \end{bmatrix} = c_s \begin{bmatrix} \mathcal{T}_{ss} \\ 0 \\ -\frac{\partial\eta}{\partial z}\mathcal{T}_{ss}. \end{bmatrix}$$

where we posed $\mathcal{T}_{ss} = \mathcal{T}_{ss}(\eta)$. In fact $T \cdot \boldsymbol{n}_\mathcal{S}$ is equal to the first column of $R\mathcal{T}$.

Relation (10) may then be rewritten componentwise as

$$\begin{cases} -p + \sigma_{rr} - \dfrac{\partial \eta}{\partial z}\sigma_{rz} = \varrho^{-1}\mathcal{T}_{ss}, \\ \sigma_{r\theta} - \dfrac{\partial \eta}{\partial z}\sigma_{\theta z} = 0, \\ \sigma_{rz} - \dfrac{\partial \eta}{\partial z}(-p + \sigma_{zz}) = \varrho^{-1}\left(-\dfrac{\partial \eta}{\partial z}\mathcal{T}_{ss}\right). \end{cases} \tag{11}$$

The term ϱ^{-1} is linked to the fact that the Navier-Stokes equations have been divided by the density. The continuity of the radial component of the velocity at the fluid-structure interface $\mathcal{S}$ implies

$$u_r = \frac{\partial \eta}{\partial t} + u_z \frac{\partial \eta}{\partial z}\,. \tag{12}$$

The Navier-Stokes equations (3) coupled with boundary conditions on $\mathcal{S}$ (11) and (12), form a consistent 3D fluid-structure interaction system (four unknowns and four boundary conditions) we will refer to throughout this paper. At this stage we will skip the problem of posing boundary conditions at the inlet and at the outlet surfaces and initial conditions. The issue will be analyzed later on for the reduced system.

2.5. **Scaling the equations.** We introduce the following scales:

$$\text{vessel length: } \quad L, \quad \text{vessel radius: } \quad R, \quad u_z\text{: } \quad V.$$

The associated dimensionless ratios are

$$\varepsilon = \frac{R}{L}, \qquad \nu = 1/Re = \frac{\mu}{VR}, \tag{13}$$

where μ is the kinematic viscosity and Re is the Reynolds number, while the corresponding derived scales are

$$u_r \text{ and } u_\theta\text{: } \quad \varepsilon V, \quad p\text{: } \quad V^2, \quad \mathcal{T}_{ss}, \mathcal{T}_{\theta\theta}, \mathcal{T}_{ll}\text{: } \quad V^2, \quad t\text{: } \quad L/V.$$

The derivation of the reduced model is based on the assumption that ε be small. With an abuse of notation that helps to reduce the number of symbols, in this section we will still denote by r, z, t, u_r, u_θ, u_z, η, p the corresponding scaled quantities. The scaled components of σ are

$$\begin{aligned} &\sigma_{rr} = 2\nu\varepsilon V^2[[D_{rr}]]\,, \quad \sigma_{\theta\theta} = 2\nu\varepsilon V^2[[D_{\theta\theta}]]\,, \quad \sigma_{zz} = 2\nu\varepsilon V^2[[D_{zz}]]\,, \\ &\sigma_{r\theta} = \varepsilon\nu V^2[[D_{r\theta}]]\,, \qquad \sigma_{z\theta} = \nu V^2[[D_{z\theta}]]\,, \quad \sigma_{rz} = \nu V^2[[D_{rz}]]\,, \end{aligned}$$

where we set

$$\begin{aligned} &[[D_{rr}]] = \frac{\partial u_r}{\partial r}\,, \qquad [[D_{rz}]] = \varepsilon^2\frac{\partial u_r}{\partial z} + \frac{\partial u_z}{\partial r}\,, \qquad [[D_{r\theta}]] = r\frac{\partial}{\partial r}\left(\frac{u_\theta}{r}\right) + \frac{1}{r}\frac{\partial u_r}{\partial \theta} \\ &[[D_{zz}]] = \frac{\partial u_z}{\partial z}\,, \qquad [[D_{z\theta}]] = \frac{1}{r}\frac{\partial u_z}{\partial \theta} + \varepsilon^2\frac{\partial u_\theta}{\partial z}\,, \qquad [[D_{\theta\theta}]] = \frac{\partial u_\theta}{\partial \theta}\frac{1}{r} + \frac{u_r}{r}\,. \end{aligned}$$

The only component of the elastic stress tensor that comes into play in the boundary conditions is $\mathcal{T}_{ss}/\varrho$, which scales as

$$\mathcal{T}_{ss}/\varrho = V^2[[\mathcal{T}_{ss}/\varrho]] \tag{14}$$

where $[[\mathcal{T}_{ss}/\varrho]]$ denotes the a-dimensional part of $\mathcal{T}_{ss}/\varrho$. Similarly we have $\mathcal{T}_{\theta\theta}/\varrho = V^2[[\mathcal{T}_{\theta\theta}/\varrho]]$ and $\mathcal{T}_{ll}/\varrho = V^2[[\mathcal{T}_{ll}/\varrho]]$.

The three-dimensional Navier-Stokes system (3) is now rewritten using the scaled quantities in order to put into evidence how the terms scale with ε. The continuity equation is formally unaltered, that is

$$\frac{\partial}{\partial r}(ru_r) + \frac{\partial u_\theta}{\partial \theta} + \frac{\partial}{\partial z}(ru_z) = 0. \tag{15}$$

After scaling and multiplication by $\dfrac{R}{V^2}$ the radial and circumferential equations become

$$\begin{aligned} \varepsilon^2 \left[\frac{\partial u_r}{\partial t} + \frac{1}{r}\frac{\partial}{\partial r}\left(ru_r^2\right) + \frac{1}{r}\frac{\partial}{\partial \theta}\left(u_r u_\theta\right) + \frac{\partial}{\partial z}(u_r u_z) - \frac{1}{r}u_\theta^2 \right] = \\ - \frac{\partial p}{\partial r} + \frac{2\nu\varepsilon}{r}\frac{\partial}{\partial r}\left(r\frac{\partial u_r}{\partial r}\right) + \frac{\nu\varepsilon}{r}\frac{\partial}{\partial \theta}\left(r\frac{\partial}{\partial r}\left(\frac{u_\theta}{r}\right) + \frac{1}{r}\frac{\partial u_z}{\partial \theta}\right) + \\ + \nu\varepsilon\frac{\partial}{\partial z}\left(\frac{\partial u_r}{\partial z}\varepsilon^2 + \frac{\partial u_z}{\partial r}\right) - \frac{2\nu\varepsilon}{r^2}\left(\frac{\partial u_\theta}{\partial \theta} + u_r\right) \end{aligned} \tag{16}$$

and

$$\begin{aligned} \varepsilon^2 \left[\frac{\partial u_\theta}{\partial t} + \frac{\partial}{\partial r}(u_r u_\theta) + \frac{1}{r}\frac{\partial}{\partial \theta}\left(u_\theta^2\right) + \frac{\partial}{\partial z}(u_\theta u_z) + \frac{2}{r}u_\theta u_r \right] = \\ - \frac{1}{r}\frac{\partial p}{\partial \theta} + \nu\varepsilon\frac{\partial}{\partial r}\left(r\frac{\partial}{\partial r}\left(\frac{u_\theta}{r}\right) + \frac{1}{r}\frac{\partial u_z}{\partial \theta}\right) + \frac{2\nu\varepsilon}{r^2}\frac{\partial}{\partial \theta}\left(\frac{\partial u_\theta}{\partial \theta} + u_r\right) + \\ + \nu\varepsilon\frac{\partial}{\partial z}\left(\frac{1}{r}\frac{\partial u_z}{\partial \theta} + \varepsilon^2\frac{\partial u_\theta}{\partial z}\right) + \frac{2\nu\varepsilon}{r}\left(r\frac{\partial}{\partial r}\left(\frac{u_\theta}{r}\right) + \frac{1}{r}\frac{\partial u_z}{\partial \theta}\right), \end{aligned} \tag{17}$$

respectively. Finally, the axial momentum equation after scaling and multiplication by L/V^2 becomes

$$\begin{aligned} \frac{\partial u_z}{\partial t} + \frac{1}{r}\frac{\partial}{\partial r}(ru_r u_z) + \frac{1}{r}\frac{\partial}{\partial \theta}(u_z u_\theta) + \frac{1}{r}\frac{\partial}{\partial z}\left(ru_z^2\right) = \\ - \frac{\partial p}{\partial z} + \frac{\nu}{\varepsilon r}\frac{\partial}{\partial r}\left[r\left(\frac{\partial u_r}{\partial z}\varepsilon^2 + \frac{\partial u_z}{\partial r}\right)\right] + \frac{\nu}{\varepsilon r}\frac{\partial}{\partial \theta}\left(\frac{1}{r}\frac{\partial u_z}{\partial \theta} + \varepsilon^2\frac{\partial u_\theta}{\partial z}\right) + 2\nu\varepsilon\frac{\partial^2 u_z}{\partial z^2}. \end{aligned} \tag{18}$$

For the derivation of our reduced model we will make use of the first of the dynamical conditions (11), which after scaling and dividing by V^2 is equivalent to

$$-p + 2\nu\varepsilon[[D_{rr}]] - \varepsilon\frac{\partial \eta}{\partial z}\nu[[D_{rz}]] = [[\mathcal{T}_{ss}/\varrho]]. \tag{19}$$

The kinematic condition (12) remains formally unaltered.

2.6. **Approximation to the first order.** We now rewrite the Navier-Stokes equations (15)–(18) neglecting all the terms which are $O(\varepsilon)$. We have

$$\begin{cases} \dfrac{\partial}{\partial r}(ru_r) + \dfrac{\partial}{\partial \theta}u_\theta + \dfrac{\partial}{\partial z}(ru_z) = 0 \\ \dfrac{\partial p}{\partial r} = \dfrac{\partial p}{\partial \theta} = 0 \\ \dfrac{\partial u_z}{\partial t} + \dfrac{1}{r}\dfrac{\partial}{\partial r}(ru_r u_z) + \dfrac{1}{r}\dfrac{\partial}{\partial \theta}(u_z u_\theta) + \dfrac{\partial}{\partial z}(u_z^2) + \\ \qquad + \dfrac{\partial p}{\partial z} - \dfrac{\nu}{r\varepsilon}\dfrac{\partial}{\partial r}\left(r\dfrac{\partial u_z}{\partial r}\right) - \dfrac{\nu}{r^2\varepsilon}\dfrac{\partial^2 u_z}{\partial \theta^2} = 0\,. \end{cases} \tag{20}$$

From (20) we infer that the pressure remains constant on each cross-section, as already pointed out in [4]. The axial momentum conservation equation gives information about the flow-convection. This is consistent with the fact that in long and thin vessels the flow develops mainly in the longitudinal direction.

The kinematic condition (12) remains identical after dropping out the terms which are $O(\varepsilon)$.

Now we evaluate with an approximation of the first order with respect to ε the component $\mathcal{T}_{ss}$ of the elastic stress tensor. We rescale (8), approximate to the first order, recover dimensions and integrate over the wall thickness. Then, we exploit relations (6). To this purpose, recalling (67) and denoting by $[[\cos\psi]]$ and by $[[\chi]]$ the rescaled expressions of $\cos\psi$ and χ, we have that:

$$[[\cos\psi]] = \left[1+\varepsilon^2\left(\frac{\partial\eta}{\partial z}\right)^2\right]^{-1/2}, \quad [[\chi]] = -\frac{\varepsilon}{L}\frac{\partial^2\eta}{\partial z^2}\left[1+\varepsilon^2\left(\frac{\partial\eta}{\partial z}\right)^2\right]^{-3/2}.$$

We remark that the previous relation in addition with the hypothesis of a small ε guarantees that h_l in (69) remains positive during motion. Therefore, with an approximation of the first order with respect to ε, relation (8) becomes:

$$\frac{\partial\left(r\mathcal{T}_{ss}\right)}{\partial s} - \mathcal{T}_{\theta\theta} = 0.$$

We now integrate for $0 \le s \le k_0$, being k_0 the thickness and recalling that $r(s) = \eta + s\cos\psi$. A zero external pressure implies that $\mathcal{T}_{ss} = 0$ outside the wall and thus we obtain that on the fluid-structure interface $\mathcal{T}_{ss}(\eta) = -\dfrac{k_0}{\eta}\mathcal{T}_{\theta\theta}(\eta)$. Since in our target applications $\eta - \eta_0$ is bounded by a quantity of the same order of magnitude as k_0 we may linearize the previous expression around $\eta = \eta_0$ and obtain

$$\mathcal{T}_{ss} = -\frac{k_0}{\eta_0}\mathcal{T}_{\theta\theta}\,. \tag{21}$$

From (6) and (21) we finally have that at the fluid-structure interface,

$$\mathcal{T}_{ss} = -\hat{\beta}_{ss}\frac{\eta-\eta_0}{\eta}, \quad \mathcal{T}_{\theta\theta} = \hat{\beta}_{\theta\theta}\frac{\eta-\eta_0}{\eta}, \quad \mathcal{T}_{ll} = \hat{\beta}_{ll}\frac{\eta-\eta_0}{\eta},$$

where

$$\hat{\beta}_{\theta\theta} = \tfrac{2G}{1-C}, \quad \hat{\beta}_{ss} = \tfrac{k_0}{\eta_0}\hat{\beta}_{\theta\theta}, \quad \hat{\beta}_{ll} = C\hat{\beta}_{\theta\theta}, \tag{22}$$

with $C = \xi\left(1-\dfrac{k_0}{\eta_0}\right)$. Remark that these quantities may be functions of z, as the Young modulus and the reference radius η_0 may vary along the longitudinal direction. They are strictly positive under the conditions $k_0/\eta_0 < 1$ (consistent with the hypothesis of a thin wall) and $\xi > 0$. We note that the relations are valid also for incompressible materials, where $\xi = 1/2$.

We remark that the negative sign in the expression for $\mathcal{T}_{ss}$ reproduces the physical fact that an expansion of the vessel corresponds to a compression of the wall structure in the radial direction. It is worth to notice that, in accordance to [15], for thin walls we have a dominance of the circumferential stress with respect to the radial stress, since in this case $\hat{\beta}_{\theta\theta} >> \hat{\beta}_{ss}$. To ease notation, in the following we will put $\beta_{ij} = \hat{\beta}_{ij}/\varrho$.

2.7. **First order approximation of the pressure.** We will calculate the pressure using the dynamic condition at the interface which expresses the equilibrium of fluid and structure forces in the radial direction. By dropping out all terms which are $O(\varepsilon)$ in (19) and recovering dimensions, we obtain that $\forall\, t \in [0,T]$ and $z \in [0,L]$,

$$p = p(\eta, z) = -\mathcal{T}_{ss}/\varrho = \beta_{ss}(z)\frac{\eta - \eta_0(z)}{\eta}. \tag{23}$$

Using (5) and (22) we obtain that

$$\beta_{ss}(z) = \frac{E(z)k_0}{\eta_0(z)\varrho\left[(1-\xi^2) + \xi(1+\xi)\frac{k_0}{\eta_0(z)}\right]}.$$

We recall that we have assumed the external pressure $p_{ext} = 0$. This is not a limitation since we can interpret p as the difference between the fluid pressure and the external pressure (what is often called *transmural* pressure). It may be convenient for further developments to introduce the quantities $A = \pi\eta^2$ and $A_0 = \pi\eta_0^2$, which represent the measure of the vessel axial section in the current and in the reference configuration, respectively. Furthermore, for the sake of notation, we will indicate in the following β_{ss} simply by β. This way, relation (23) may be written in the form

$$p = \beta\left(1 - \sqrt{\frac{A_0}{A}}\right), \quad \text{where } \beta = \frac{Ek_0\sqrt{\pi}}{\varrho\sqrt{A_0}\left[(1-\xi^2) + \xi(1+\xi)\frac{k_0\sqrt{\pi}}{\sqrt{A_0}}\right]}. \tag{24}$$

With respect to the expression proposed in [23], which may be rewritten in the form

$$p = \beta_0\left(\sqrt{\frac{A}{A_0}} - 1\right), \quad \text{with } \beta_0 = \frac{Ek_0\sqrt{\pi}}{\varrho\sqrt{A_0}(1-\xi^2)}, \tag{25}$$

the differences are that (25) has been obtained through a linearization procedure and that the expression for β accounts also for a moderately thick vessel wall, while β_0 neglects terms of the order of k_0/η_0. The latter difference is however, less relevant and may be neglected. It is easy to verify that the expression for the pressure given in (24) satisfies the hypothesis of admissibility illustrated in [23], namely that $p = 0$ whenever $\eta = \eta_0$ (remember that here p is the transmural pressure) and $\frac{\partial p}{\partial A} > 0$ for all $A > 0$.

Remark 1. Expression (25) may be formally obtained from (24) by neglecting the term proportional to k_0/η_0 and taking a Young modulus function of η, namely $E = \bar{E}\frac{\sqrt{A}}{\sqrt{A_0}}$, being $\bar{E}$ a constant (possibly depending on z). This can be justified to account for large arteries which tend to stiffen when expanded. We point out that this is just an heuristic remark: a variable elastic parameter would imply a non-linear elastic constitutive equation and require us to revise the whole derivation of the simplified model. However, it helps to explain why a formally less correct formula is so used in practice for haemodynamic simulations.

To broad our analysis to cover different possible pressure-area relationships, we will consider a general relation of the type

$$p(A, z) = C(z)\left[\left(\frac{A}{A_0(z)}\right)^{d(z)} - 1\right], \tag{26}$$

where $C(z)$ and $d(z)$ are known parameters which satisfy $C(z)d(z) > 0$ and $|d| < 2$. We obtain, as special cases, (24) by setting $C(z) = -\beta(z)$ and $d(z) = -\frac{1}{2}$, and (25) by setting $C(z) = \beta_0(z)$ and $d(z) = \frac{1}{2}$.

3. **The 1D-reduced fluid-structure-interaction model.** In this section we derive a one-dimensional model, performing term by term cross-section integration of the continuity equation and of the longitudinal momentum equation in (20). The pressure is assigned through formula (23). We will use the following notation.

Notation. Let $f : [0,T] \times \mathbb{R}^+ \times [0,2\pi) \times [0,L] \to \mathbb{R}$. Then:

$$\bar{f}(t,z) \doteq \int_0^{2\pi} \int_0^{\eta} f(t,r,\theta,z) r dr d\theta, \quad \overline{\overline{f}}(t,z) \doteq \frac{1}{\pi\eta^2} \bar{f}(t,z)\,.$$

Remark 2. Observe that, if $g : [0,T] \times \mathbb{R}^+ \times [0,2\pi) \times [0,L] \to \mathbb{R}$ is a sufficiently smooth function, the following identities hold:

$$\overline{\frac{\partial g}{\partial t}} \;=\; \frac{\partial \overline{g}}{\partial t} \;-\; \eta \frac{\partial \eta}{\partial t} \int_0^{2\pi} g_{|r=\eta} d\theta, \quad \overline{\left(\frac{1}{r}\frac{\partial (rg)}{\partial r}\right)} \;=\; \eta \int_0^{2\pi} g_{|r=\eta}\, d\theta\,.$$

Moreover, if g is continuous w.r.t. the coordinate θ, for any $\alpha \in \mathbb{R}$ we have

$$\overline{\left(r^\alpha \frac{\partial g}{\partial \theta}\right)} = \int_0^{\eta} r^{\alpha+1} \left(\int_0^{2\pi} \frac{\partial g}{\partial \theta}\, d\theta\right) dr = 0 \quad \text{and}$$
$$\overline{\left(r^\alpha \frac{\partial g}{\partial z}\right)} = \frac{\partial}{\partial z}\overline{g r^\alpha} - \eta^{\alpha+1} \frac{\partial \eta}{\partial z} \int_0^{2\pi} g_{|r=\eta}\, d\theta\,.$$

Let us consider the continuity equation in (20) and average each term on the cross-section. Then, using the expressions in Remark 2 and taking (12) we obtain that

$$\frac{\partial(\eta^2)}{\partial t} + \frac{\partial(\eta^2 \overline{\overline{u_z}})}{\partial z} = 0. \tag{27}$$

3.1. **Assumptions on the velocity profile.** We will assume that

$$\overline{\overline{u_z}}^2(t,z) - \overline{\overline{u_z^2}}(t,z) = O(\varepsilon).$$

This implies that the velocity profile is mainly flat.

Remark 3. Sometimes one accounts for a different velocity profile by introducing a coefficient in the quadratic advective term, the so-called momentum correction coefficient, like in [23]. However, this is not the route we have followed here. Indeed, the correct value of the coefficient is difficult to find in general. Moreover, in practice, it has been found that in haemodinamic applications its value would be proximal to one [25], and its influence in the solution is negligible.

3.2. **Averaging the axial momentum equation.** Let us first consider the convective term of the axial momentum equation in (20) and average each term on the cross-section. Then, thanks to Remark 2, taking (12) into account, in view of the assumption on the velocity and dropping out the terms which are $O(\varepsilon)$, we may write

$$\frac{\partial(\eta^2 \overline{\overline{u_z}})}{\partial t} + \frac{\partial\left(\eta^2 \overline{\overline{u_z^2}}\right)}{\partial z} = \frac{\partial(\eta^2 \overline{\overline{u_z}})}{\partial t} + \frac{\partial\left(\eta^2 \overline{\overline{u_z}}^2\right)}{\partial z}. \tag{28}$$

The remaining terms after averaging give

$$\frac{\partial}{\partial z}\int_0^{2\pi}\int_0^{\eta} prdrd\theta - \int_0^{2\pi}\eta\left[\frac{\partial \eta}{\partial z}p + \nu\frac{\partial u_z}{\partial r}\frac{1}{\varepsilon}\right]_{|r=\eta} \quad d\theta \tag{29}$$

The last term in the previous expression will be modelled as in [4, 25] and [23] by assuming that the velocity in cylindrical coordinates of the form $u_z(t,r,z) = \overline{\overline{u_z}}(t,z)s(r/\eta)$, with s a suitable chosen profile satisfying $s'(1) < 0$. This hypothesis is akin to that used for the shallow water equations and gives rise to a friction term [9]. More precisely, we assume that

$$\int_0^{2\pi}\eta\nu\ \frac{\partial u_z}{\partial r}\frac{1}{\varepsilon}\Big]_{|r=\eta} \quad d\theta \simeq -\frac{2\pi}{\varepsilon}\nu\gamma\overline{\overline{u_z}} = -K_\varepsilon\overline{\overline{u_z}}, \tag{30}$$

where $K_\varepsilon = \frac{2\pi}{\varepsilon}\nu\gamma$ and the positive constant γ depends on the particular velocity profile chosen. Typically γ may vary from 4 to around 20. For instance in [25] the authors adopt a profile to fit the experimental data which gives $\gamma = 11$. By taking into account the fact that the pressure is considered constant on each section, thanks to relation (26), the term (29) becomes

$$\pi\eta^2\frac{\partial p}{\partial z} + K_\varepsilon\overline{\overline{u_z}}. \tag{31}$$

Remark 4. The size of the coefficient K_ε in the friction term becomes arbitrarily large as $\varepsilon \to 0$. It is important then to assess its relative importance for the application to hand. If we consider relation (26) in the hypothesis of constant coefficients, the terms in the expression (31) may be rewritten as (we recall that we are still considering the scaled variables)

$$\frac{c_1^2}{V^2}\frac{\partial A}{\partial z} + K_\varepsilon\overline{\overline{u_z}}.$$

Here, $A = \pi\eta^2$ is the (scaled) section measure while $c_1^2 = A\dfrac{\partial p}{\partial A}$ is the square of a characteristic speed whose significance will be made clear in the next paragraph. The latter does not depend on ε if we consider pressure laws of the type (24) or (25), under the reasonable assumption that the ratio $k_0/\sqrt{A_0}$ is independent of ε.

We can then consider that the friction term is not dominant whenever $K_\varepsilon \leq \frac{c_1^2}{V^2}$, i.e. $\frac{2\pi\gamma V^2}{c_1^2\varepsilon Re} \leq 1$ (we recall that here $\nu = Re^{-1}$). In the case of blood flow in large and medium sized arteries, which is the target application of this work, we have that $Re \simeq 100 - 1000$, $c_1 \simeq 1 - 10\ m/s$, $V \simeq 10^{-2} - 10^{-1}\ m/s$ and $\varepsilon \simeq 0.01 - 0.1$. Therefore, here the inequality is largely satisfied.

In fact, in this case the viscous term is rather small. This justifies the fact that in many studies of blood flow in arteries, friction is neglected [4, 22]. Indeed numerical studies [19] have shown that the introduction of the friction term does not change the behavior of the solution significantly.

For the sake of notation we will indicate in the following $u = \overline{\overline{u_z}}$.

3.3. **The 1D model.** Recovering dimensions, in terms of the variables A and

$$Q \doteq \pi\eta^2 u = Au\,,$$

after simple computations we obtain the following reduced model on $(0,T)\times(0,L)$:

$$\begin{cases} \dfrac{\partial A}{\partial t}+\dfrac{\partial Q}{\partial z}=0 \\ \dfrac{\partial Q}{\partial t}+\dfrac{\partial}{\partial z}\left(\dfrac{Q^2}{A}\right)+A\dfrac{\partial p}{\partial z}+K\dfrac{Q}{A}=0 \\ p(A,z)=C(z)\left[\left(\dfrac{A}{A_0(z)}\right)^{d(z)}-1\right] \end{cases} \tag{32}$$

with $K=2\pi\mu\gamma$ being the friction constant, while $d(z)$ and $C(z)$, are subject to the limitations stated in Remark 1.

We will see in the next section that system (32) is hyperbolic and that for our target application the associated eigenvalues have different signs. This implies that a single boundary condition should be imposed at $z=0$ and $z=L$, respectively. In haemodynamic applications we normally distinguish between proximal and distal boundaries. A proximal boundary corresponds to the axial section of the artery nearer to the heart, the distal boundary is instead the farther. Since the action driving the flow is coming from the heart, in the proximal boundary one normally prescribes either velocity or pressure, obtained from measurements or available medical literature. The proximal boundary is more critical because it is at the interface with the peripheral circulation. Several approaches can be followed. A possibility is to impose 'non-reflecting' boundary conditions, since these conditions will not allow any spurious reflection at the boundary. In fact, from a physical point of view this corresponds to an open end. However, a more realistic action of the peripheral circulation is accounted for by a resistance relation of the type $p=Ru$, being R a given resistance parameter. In [24] it is shown how this relation can in fact be expressed in terms of the characteristic variables of system (32), and this is indeed the form we consider in the sequel, where we will assume that $z=0$ and $z=L$ are the proximal and the distal boundaries, respectively.

We mention that more complex boundary relations may be considered to better account of the global action of the circulatory system, where the boundary data is governed by ordinary differential equations [13, 11], a case that will not be covered here.

4. Mathematical analysis.

In this section we write a conservation form and point out some analytical properties of the system (32). Then, in the constant coefficients case and assuming $K=0$, we consider the initial boundary value problem on a finite space with suitable boundary conditions and discuss the existence of regular solutions which are defined globally in time.

4.1. The conservation form.

In terms of variables A, Q, the system (32) in conservation form is given by:

$$\begin{cases} \dfrac{\partial A}{\partial t} + \dfrac{\partial Q}{\partial z}=0 \\ \dfrac{\partial Q}{\partial t} + \dfrac{\partial}{\partial z}\left(\dfrac{Q^2}{A}+\dfrac{Cd}{A_0^d(d+1)}A^{d+1}\right)=S(z,A)-K\dfrac{Q}{A} \end{cases} \tag{33}$$

where $Cd>0$, $|d|<2$, $d\neq -1$, $A>0$, $A_0>0$. The source term S depends on the known parameters $C(z)$, $d(z)$, $A_0(z)$ and vanishes if these parameters are constant.

Its explicit form may be derived following the computations illustrated in [23]. If we use expression (24) for the pressure term, the source term becomes

$$S(z,A) = \beta\sqrt{\frac{A}{A_0}}\frac{dA_0}{dz} + \sqrt{A}\left(2\sqrt{A_0} - \sqrt{A}\right)\frac{d\beta}{dz}\,.$$

4.2. **The eigenvalues.** The Jacobian of the flux in the system (33) is given by:

$$\begin{bmatrix} 0 & 1 \\ -\dfrac{Q^2}{A^2} + c_1^2 & \dfrac{2Q}{A} \end{bmatrix}; \tag{34}$$

its eigenvalues are given by $\gamma = u - c_1$, $\mu = u + c_1$, where

$$c_1(z,A) = \left[A\frac{\partial p}{\partial A}\right]^{1/2} = \sqrt{Cd}\left(\frac{A}{A_0}\right)^{\frac{d}{2}}. \tag{35}$$

The quantity c_1 in (35) has already been introduced in Remark 4 and is a *characteristic speed* of our system. Since we required $Cd > 0$, the eigenvalues are well defined for $A, A_0 > 0$ and real with $\mu > \gamma$ and then (33) is strictly hyperbolic. Moreover, the system is genuinely nonlinear. Indeed we have that

$$R_\gamma = -[1,\gamma]^t, \qquad R_\mu = [1,\mu]^t$$

are right eigenvectors of (34); then, setting $U = [A,Q]^t$, we obtain

$$\nabla_U\gamma\cdot R_\gamma = \nabla_U\mu\cdot R_\mu = \frac{\partial c_1}{\partial A} + \frac{c_1}{A} = \frac{c_1}{A}\left(1+\frac{d}{2}\right) > 0 \quad \text{since } |d| < 2\,.$$

4.3. **The Riemann invariants.** Following [6], chap. VII, we compute the two Riemann invariants associated to the system (33), as the scalar functions $r(z,U)$, $s(z,U)$ such that:

$$\frac{\partial r}{\partial U} = L_\gamma, \quad \frac{\partial s}{\partial U} = L_\mu$$

where L_γ, L_μ are the left eigenvectors of the matrix (34):

$$L_\gamma(z,A,u) = [-\mu,1]\xi(A,Q), \qquad L_\mu(z,A,u) = [-\gamma,1]\xi(A,Q)$$

and $\xi(A,Q)$ is a scalar smooth function of its arguments. Choosing $\xi(A,Q) = 1/A$ we find

$$r(z,U) = u - F\,, \qquad s(z,U) = u + F\,, \tag{36}$$

where

$$F = F(z,A) = \int_{A_0}^{A}\frac{c_1(z,\alpha)}{\alpha}\,d\alpha = \frac{2}{d}\big(c_1(z,A) - c_1(z,A_0(z))\big)\,. \tag{37}$$

Here we used the fact that $\frac{c_1}{A} = \frac{2}{d}\cdot\frac{\partial c_1}{\partial A}$. Observe that $\partial F/\partial A > 0$. Using (36) and (37), we can express u, c_1 and then γ, μ in terms of r, s:

$$u = \frac{r+s}{2}\,, \qquad c_1 = \frac{d}{4}(s-r) + \sqrt{Cd}\,,$$

$$\gamma = \frac{r(2+d)+s(2-d)}{4} - \sqrt{Cd}\,, \qquad \mu = \frac{r(2-d)+s(2+d)}{4} + \sqrt{Cd}\,. \tag{38}$$

Observe that it must be $c_1 > 0$; this gives a constraint on r, s. In Riemann coordinates, the system (33) rewrites as

$$\frac{\partial r}{\partial t} + \gamma(z,r,s)\frac{\partial r}{\partial z} = E_1(z,r,s)\,, \qquad \frac{\partial s}{\partial t} + \mu(z,r,s)\frac{\partial s}{\partial z} = E_2(z,r,s)$$

with suitable E_1 and E_2.

4.4. **The special case where $K = 0$ and the parameters are constant.** From now on, we assume that the parameters A_0, C and d are constant. Furthermore, following Remark 4 we neglect the friction term. Therefore, the source terms in (33) vanish and the system becomes homogeneous. We then consider an initial–boundary value problem on the interval $[0, L]$ for the system

$$\begin{cases} \dfrac{\partial A}{\partial t} + \dfrac{\partial Q}{\partial z} = 0 \\ \dfrac{\partial Q}{\partial t} + \dfrac{\partial}{\partial z}\left(\dfrac{Q^2}{A} + \dfrac{Cd}{A_0^d(d+1)}A^{d+1}\right) = 0 \end{cases} \tag{39}$$

where C, $d \neq -1$ and A_0 are constant, $Cd > 0$, provided with initial data

$$A(0, z) = A_0, \qquad u(0, z) = u_0(z), \qquad z \in [0, L]\,. \tag{40}$$

As for the boundary conditions, we prescribe at $z = 0$ either the vessel area $A(0, t) = A_{in}(t)$ (which is in fact equivalent to impose the pressure) or the velocity $u(0, t) = u_{in}(t)$, while at the outlet boundary $z = L$ we impose that $r = -ks$, where $k \in [0, 1)$.

The latter condition is used to simulate the presence of a resistance to the flow. If $k = 0$ we have a non reflecting condition which physically coincides with an open ending. The limit case $k = 1$ instead corresponds to $u = 0$, and therefore to a complete blockage. Indeed, we can link k to the resistance R in the classical relation $p = Ru$ at $z = L$ [24]. By simple computations, assuming that $|r - s|$ is small (which is the case here), we have $R \simeq \frac{1+k}{1-k} c_1(A_0)$.

To summarize, we consider either

$$z = 0: \quad A(t, 0) = A_{in}(t)\,, \qquad z = L: \qquad u - \alpha F(A) = 0\,, \tag{41}$$

or

$$z = 0: \qquad u(t, 0) = u_{in}(t)\,, \qquad z = L: \qquad u - \alpha F(A) = 0\,, \tag{42}$$

where $\alpha = \frac{1-k}{1+k}$, $0 < \alpha \leq 1$, $0 \leq k < 1$, and

$$F(A) = F(A; A_0) = \frac{2\sqrt{Cd}}{d}\left[\left(\frac{A}{A_0}\right)^{\frac{d}{2}} - 1\right].$$

We point out that, if $d > 0$, the system (39) reduces to the classical p-system of gas-dynamics with exponent $d + 1$. In diagonal coordinates, the system can be rewritten as

$$\frac{\partial r}{\partial t} + \gamma(r, s)\frac{\partial r}{\partial z} = 0\,, \qquad \frac{\partial s}{\partial t} + \mu(r, s)\frac{\partial s}{\partial z} = 0\,. \tag{43}$$

Since $F(A_0) = 0$, the initial data for r, s are

$$r(0, z) = s(0, z) = u_0(z)\,, \qquad z \in [0, L] \tag{44}$$

while the boundary conditions (41), (42) become, respectively

$$z = 0: \quad s = r + v\,, \quad v(t) = 2F\left(A_{in}(t)\right)\,, \quad z = L: \qquad r = -ks \tag{45}$$

$$z = 0: \quad s = -r + v\,, \quad v(t) = 2u_{in}(t)\,, \qquad z = L: \qquad r = -ks\,. \tag{46}$$

We analyze the above IBV problems for (43) with smooth data. For the Cauchy problem, in general, classical solutions exist only locally in time, since the first order derivatives may blow up, even for arbitrarily small data ([1], [18], [21]).

On the other hand, on a fixed bounded domain, smooth solutions may exist if the boundary conditions are suitably dissipative ([17], [20]). See [3] for a review on the subject and for a classification of possible behaviors of the solutions in presence of boundary damping but not-too-small data.

The problem studied here falls within the framework considered in [20], Chapter 5, Th. 1.1. The result is the following.

Theorem 1. *([20]) Consider the system (43) with initial data r_0, s_0 and b.c.*

$$z=0: \qquad s=g(r)+v(t)\,, \qquad\qquad z=L: \qquad r=f(s)\,.$$

Assume that γ, μ, f, g, r_0, s_0 are C^1 and that the C^1 compatibility conditions

$$z=0: \quad \begin{cases} s_0(0)=g(r_0(0))+v(0) \\ \mu(r_0(0),s_0(0))s_0'(0)=g'(r_0(0))\gamma(r_0(0),s_0(0))r_0'(0)-v'(0) \end{cases}$$

$$z=L: \quad \begin{cases} r_0(L)=f(s_0(L)), \\ \gamma(r_0(L),s_0(L))r_0'(L)=f'(s_0(L))\mu(r_0(L),s_0(L))s_0'(L) \end{cases}$$

are satisfied with $\gamma(0,0)<0<\mu(0,0)$, $f(0)=g(0)=0$ and $|f'(0)g'(0)|<1$.

Then there exists $\varepsilon_o>0$ such that: for all $0<\varepsilon\le\varepsilon_o$ there exists $\delta=\delta(\varepsilon)$ such that, if $\|v\|_{C^1}$, $\|r_0\|_{C^1}$, $\|s_0\|_{C^1}$ are less than δ, then the IBV problem above admits a C^1 solution on $[0,+\infty)\times[0,L]$. Moreover, $\|(r,s)(t,\cdot)\|_{C^1}\le\varepsilon$.

In our case, $g(r)=\pm r$ and $f(s)=-ks$, thus $|f'(0)g'(0)|=k<1$. Since we are interested in having explicit bounds on the data, we give a proof of Theorem 1 suited for our problem.

Proposition 1. **(I)** *Let $A_{in}:[0,+\infty)\to\mathbb{R}^+$ be of class C^1, $A_0>0$, $u_0\in C^1([0,L])$ and assume the following compatibility conditions:*

$$A_{in}(0)=A_0, \qquad A_0u_0'(0)+A_{in}'(0)=0, \qquad u_0(L)=u_0'(L)=0\,. \tag{47}$$

Moreover, set $v(t)=2F(A_{in}(t))$. Assume that

$$\|u_0\|_{C^0([0,L])}+\frac{1}{1-k}\|v\|_{C^0([0,\infty))} \;<\; \frac{1-\sqrt{k}}{1+\sqrt{k}}\sqrt{Cd} \tag{48}$$

and that

$$b_o \;=\; \max\{\|u_0'\|_{C^0([0,L])},\ \|v'\|_{C^0([0,\infty))}\} \tag{49}$$

is sufficiently small (see (55) below). Then the IBV problem (39)–(41) admits a unique C^1 solution $(A(t,z),u(t,z))$ on $[0,\infty)\times[0,L]$.

(II) *Let $u_{in}\in C^1([0,+\infty))$, $A_0>0$, $u_0\in C^1([0,L])$, and assume the compatibility conditions*

$$u_{in}(0)=u_0(0), \qquad u_0(0)u_0'(0)+u_{in}'(0)=0, \qquad u_0(L)=u_0'(L)=0\,. \tag{50}$$

Moreover, set $v(t)=2u_{in}(t)$. Assume (48) and that b_o, defined at (49), is sufficiently small (see (55) below).

Then the same conclusion of **(I)** *holds for the IBV problem (39), (40), (42).*

Proof. We consider the problem in Riemann coordinates, (43)–(45) for case **(I)** and (43), (44), (46) for case **(II)**. The eigenvalues at $t=0$ are given by

$$\gamma_0(z)=u_0(z)-\sqrt{Cd}\,, \qquad \mu_0(z)=u_0(z)+\sqrt{Cd}\,.$$

The C^1 compatibility conditions here become

$$\begin{array}{lll} \textbf{(I)}, \quad z=0: & F\left(A_{in}(0)\right)=0\,, & \left(\mu_0(0)-\gamma_0(0)\right)u_0'(0)+2F'(A_0)A_{in}'(0)=0 \\ \textbf{(II)}, \quad z=0: & u_0(0)=u_{in}(0)\,, & \left(\mu_0(0)+\gamma_0(0)\right)u_0'(0)+2u_{in}'(0)=0 \\ z=L: & u_0(L)=0\,, & \left(\gamma_0(L)+k\mu_0(L)\right)u_0'(L)=0 \end{array}$$

that easily follow from (47), (50).

The existence and uniqueness of a local in time C^1 solution is guaranteed by classical results. Let us now seek the a priori estimates on r, s and their derivatives.

Estimates on r, s. Recall that r is constant along γ-characteristics and s is constant along μ-characteristics. Consider the μ-characteristics issued at the left corner $(t=0, z=0)$. Assuming that the solution exists long enough, the characteristics will reach the right boundary at a time t_1; at that point, a γ-characteristics is issued and it will reach the boundary $z=0$ at a time T_2, and so on. Let $\{t_{2j-1}\}_{j=1,2,\dots}$ and $\{T_{2j}\}_{j=1,2,\dots}$ be the sequences of increasing times at which the μ-characteristics issued at $(0,0)$ hits the boundary $z=L$ and $z=0$, respectively.

Similarly, consider the γ-characteristics issued at $(t=0, z=L)$. It will reach the boundary line $z=0$ at a time T_1, then a μ-characteristics is issued at that point, and so on. Let $\{T_{2j-1}\}_{j=1,2,\dots}$ and $\{t_{2j}\}_{j=1,2,\dots}$ be the sequences of increasing times at which the γ-characteristics issued at $(0,L)$ hits the boundary $z=0$ and $z=L$, respectively. Finally, set $t_0=T_0=0$.

One can verify easily that the sequences $\{T_j\}_{j\in\mathbb{N}}$, $\{t_j\}_{j\in\mathbb{N}}$ are strictly increasing, as soon as the solution is C^1. Define

$$R_j=\max_{[T_j,T_{j+1}]}|r(t,0)|\,,\qquad S_j=\max_{[t_j,t_{j+1}]}|s(t,L)|\,,\qquad j=0,1,\dots\,.$$

Recalling (44), one has

$$R_0=\max_{z\in[0,L]}|r(0,z)|=\|u_0\|_{C^0([0,L])}=\max_{z\in[0,L]}|s(0,z)|=S_0$$

and, in both cases **(I)**, **(II)**

$$R_{j+1}\le kS_j\,,\qquad S_{j+1}\le R_j+V\,,\qquad j=0,1,\dots$$

where $V=\|v\|_{C^0([0,\infty))}$. Iterating the above formulas, one gets

$$R_{j+1}\le kR_{j-1}+kV\,,\qquad S_{j+1}\le kS_{j-1}+V\,,\qquad j=1,2,\dots$$

Hence one has $R_1\le kS_0\le R_0$ and for all $j\ge 1$

$$R_{2j}\le k^jR_0+\frac{kV}{1-k},\qquad R_{2j+1}\le k^jR_1+\frac{kV}{1-k}$$

and we obtain

$$\max\{R_{2j},R_{2j+1}\}\le k^jR_0+\frac{kV}{1-k}\,,\qquad j=1,2,\dots$$

Similarly, one has $S_1\le R_0+V=S_0+V$. Then for all $j\ge 1$

$$\begin{aligned} S_{2j} &\le k^jS_0+\frac{V}{1-k}\,, \\ S_{2j+1} &\le k^jS_1+V\sum_{\ell=0}^{j-1}k^\ell \;\le\; k^jS_0+V\sum_{\ell=0}^{j}k^\ell\,, \end{aligned}$$

hence we obtain

$$\max\{S_{2j},S_{2j+1}\}\le k^jS_0+\frac{V}{1-k},\qquad j=1,2,\dots$$

Now we can easily get global bounds on r, s. Indeed

$$\max_{\ell\geq 0} R_\ell \leq \max\left\{R_0,\ kR_0+\frac{kV}{1-k}\right\} \doteq \tilde R$$
$$\max_{\ell\geq 0} S_\ell \leq \max\left\{S_0+V,\ kS_0+\frac{V}{1-k}\right\} \doteq \tilde S\,.$$

If $k=0$, then $\tilde R = R_0$, $\tilde S = S_0+V$, while for $k\to 1^-$ the second term prevails. In conclusion, as soon as the C^1 solution exists, one has $|r(t,z)|\leq \tilde R$, $|s(t,z)|\leq \tilde S$. Observe that $\tilde R\leq \tilde S\leq S_0+\frac{V}{1-k}$. Now, we claim that if (48) hold, that is, if

$$S_0+\frac{V}{1-k} < \frac{1-\sqrt{k}}{1+\sqrt{k}}\sqrt{Cd} \leq \sqrt{Cd}\,,$$

then A is well defined and the eigenvalues do not change sign. Indeed one has

$$\frac{r(2+d)+s(2-d)}{4} \leq \tilde S \ <\ \sqrt{Cd}\,, \qquad \frac{r(2-d)+s(2+d)}{4} \geq -\tilde S \ >\ -\sqrt{Cd}$$

which implies, by recalling (38), that $\gamma<0<\mu$. To show that A is well defined, we need to invert F. We recall that F is strictly increasing; moreover, if $d<0$ $F(A)\to -\infty$ as $A\to 0+$ and $F(A)\to 2\sqrt{C/d}$ as $A\to+\infty$, while if $d>0$ $F(A)\to+\infty$ as $A\to+\infty$, and $F(A)\to -2\sqrt{C/d}$ as $A\to 0+$. Since $|d|<2$ and $Cd>0$, we have

$$|F(A)| = \left|\frac{s-r}{2}\right| \ \leq\ \tilde S < \ \sqrt{Cd}\ <\ 2\sqrt{\frac{C}{d}}\,,$$

then we deduce that A is well defined and is bounded away from 0.

Estimates on $\partial_z r$, $\partial_z s$. Define

$$h(r,s) = \frac{d-2}{2d}\log\left(\frac{c_1(r,s)}{c_1(r,r)}\right) = \frac{d-2}{2d}\log\left(1+\frac{d(s-r)}{4\sqrt{Cd}}\right)\,.$$

This function has the following properties: $h|_{r=s}=0$,

$$\frac{\partial h}{\partial r} = -\frac{\partial h}{\partial s} = \frac{1}{\mu-\gamma}\frac{\partial \gamma}{\partial s} = \frac{1}{\mu-\gamma}\frac{\partial \mu}{\partial r}\,.$$

Hence the functions

$$U = e^{h(r,s)}\frac{\partial r}{\partial z}\,, \qquad V = e^{h(r,s)}\frac{\partial s}{\partial z}$$

satisfy, recalling that $\partial\gamma/\partial r = \partial\mu/\partial s = (2+d)/4$,

$$\begin{cases} (\partial_t+\gamma(r,s)\partial_z)\,U \ =\ -\frac{2+d}{4}e^{-h(r,s)}U^2\,,\\ (\partial_t+\mu(r,s)\partial_z)\,V \ =\ -\frac{2+d}{4}e^{-h(r,s)}V^2\,. \end{cases}$$

with initial condition $U(0,z)=r_z(0,z)=u_0'(z)$, $V(0,z)=s_z(0,z)=u_0'(z)$ and b.c.

$$z=0: \qquad V=\frac{\gamma}{\mu}U-\frac{e^h}{\mu}v'(t)\,, \qquad\qquad z=L: \qquad U=k\frac{\mu}{|\gamma|}V\,, \tag{51}$$

in case **(I)**, while in case **(II)**

$$z=0: \qquad V=\frac{|\gamma|}{\mu}U-\frac{e^h}{\mu}v'(t)\,, \qquad\qquad z=L: \qquad U=k\frac{\mu}{|\gamma|}V\,. \tag{52}$$

Assumptions on the data. We observe again that, thanks to (48), one has $\tilde{S} < \sqrt{Cd}(1-\sqrt{k})/(1+\sqrt{k})$. Hence there exists a constant $\alpha > 0$ such that

$$k\left(\frac{\sqrt{Cd}+\tilde{S}}{\sqrt{Cd}-\tilde{S}}\right)^2 < \alpha^2 < 1\,. \tag{53}$$

Clearly, if we set

$$M_1 \;=\; \max_{|r|,|s|\le\tilde{S}} \mu/|\gamma| = \max_{|r|,|s|\le\tilde{S}} |\gamma|/\mu \;=\; \frac{\sqrt{Cd}+\tilde{S}}{\sqrt{Cd}-\tilde{S}}\,,$$

we have

$$\beta \doteq \frac{kM_1^2}{\alpha^2} \;\in\; [0,1)\,. \tag{54}$$

Our main assumption on b_o, the quantity defined at (49), is that

$$b_o \;\le\; \frac{1}{B(M_1+2M_2)} \max_{\sqrt{k}M_1\le\alpha\le 1} \alpha(1-\alpha)(1-\beta) \tag{55}$$

where

$$B \;=\; L\cdot\frac{2+d}{4}\cdot \max_{|r|,|s|\le\tilde{S}} \left\{\frac{1}{\mu}, \frac{1}{|\gamma|}\right\}\cdot \max_{|r|,|s|\le\tilde{S}} e^{-h(r,s)}\,,$$

$$M_2 \;=\; \max_{|r|,|s|\le\tilde{S}} \frac{e^{h(r,s)}}{\mu(r,s)}\,.$$

In the following, we choose $\alpha \in (\sqrt{k}M_1, 1)$ such that the maximum in (55) is attained.

Iterative estimates. Now define

$$\mathcal{U}_j = \max_{[T_j,T_{j+1}]} |U(t,0)|\,, \qquad \mathcal{V}_j = \max_{[t_j,t_{j+1}]} |V(t,L)|\,, \qquad j\ge 0\,.$$

Let $t\in[0,T_1]$. Solving the Riccati equation, one finds

$$U(t,0) = U(0,\xi)\cdot\left[1+U(0,\xi)\frac{2+d}{4}\int_0^t e^{-h(\tau)}\,d\tau\right]^{-1}$$

for some $\xi\in[0,L]$; here h is evaluated along the γ-characteristics joining $(0,\xi)$ with $(t,0)$. After (55), one has $b_oB\le 1-\alpha$, hence

$$|U(t,0)| \le \frac{|U(0,\xi)|}{1-|U(0,\xi)|B} \le \frac{b_o}{1-b_oB} \le \frac{b_o}{\alpha}\,.$$

The argument for V is similar. Hence one has $\mathcal{U}_0,\ \mathcal{V}_0 \le b_o/\alpha$. Now let $t\in[T_1,T_2]$. Using (51), one finds

$$U(t,0) = k\frac{\mu}{|\gamma|}V(\tilde{t},L)\cdot\left[1+k\frac{\mu}{|\gamma|}V(\tilde{t},L)\frac{2+d}{4}\int_{\tilde{t}}^t e^{-h(\tau)}\,d\tau\right]^{-1}$$

for some $\tilde{t}\in[0,t_1]$. Hence

$$\mathcal{U}_1 \le \frac{kM_1|V(\tilde{t},L)|}{1-kM_1|V(\tilde{t},L)|B} \;\le\; \frac{kM_1\mathcal{V}_0}{1-kM_1\mathcal{V}_0B} \qquad \text{if } \mathcal{V}_0BkM_1<1\,.$$

Similarly, one finds for $j\ge 0$

$$\mathcal{U}_{j+1} \;\le\; \frac{kM_1\mathcal{V}_j}{1-kM_1\mathcal{V}_jB} \qquad \text{provided that } \mathcal{V}_jkM_1B<1\,. \tag{56}$$

Now, let us give estimates on $\mathcal{V}_j$, $j = 1, 2, \ldots$. Let $t \in [t_1, t_2]$, then

$$V(t, L) = V(\tilde{t}, 0) \cdot \left[1 + V(\tilde{t}, 0) \frac{2+d}{4} \int_{\tilde{t}}^{t} e^{-h(\tau)}\, d\tau \right]^{-1}$$

for some $\tilde{t} \in [0, T_1]$, where now h is evaluated along the μ-characteristics joining $(\tilde{t}, 0)$ with (t, L). Using (51), (52), one finds

$$|V(\tilde{t}, 0)| \;\leq\; M_1 \mathcal{U}_0 \;+\; M_2 b_o\,,$$

hence

$$\mathcal{V}_1 \leq \frac{M_1 \mathcal{U}_0 \;+\; M_2 b_o}{1 - (M_1 \mathcal{U}_0 \;+\; M_2 b_o)\, B}\,, \qquad (M_1 \mathcal{U}_0 \;+\; M_2 b_o)\, B < 1$$

and, for $j = 0, 1, \ldots$

$$\mathcal{V}_{j+1} \leq \frac{M_1 \mathcal{U}_j \;+\; M_2 b_o}{1 - (M_1 \mathcal{U}_j \;+\; M_2 b_o)\, B} \qquad \text{provided that } (M_1 \mathcal{U}_j \;+\; M_2 b_o)\, B < 1\,. \quad (57)$$

For the moment, assume that

$$\mathcal{V}_j k M_1 B \;\leq\; 1 - \alpha \qquad j \geq 0 \quad (58)$$

$$(M_1 \mathcal{U}_j \;+\; M_2 b_o)\, B \;\leq\; 1 - \alpha \qquad j \geq 0\,. \quad (59)$$

These assumptions will be justified later. Hence from (56), (57) we get

$$\mathcal{U}_{j+1} \;\leq\; \frac{k M_1}{\alpha} \mathcal{V}_j\,, \qquad \mathcal{V}_{j+1} \leq \frac{M_1}{\alpha} \mathcal{U}_j \;+\; \frac{M_2}{\alpha} b_o\,, \qquad j \geq 0\,. \quad (60)$$

Iterating the above formulas, and recalling (54), we get

$$\mathcal{U}_{j+1} \;\leq\; \beta \mathcal{U}_{j-1} \;+\; \frac{k M_1 M_2}{\alpha^2}\, b_o\,, \qquad \mathcal{V}_{j+1} \leq \beta\, \mathcal{V}_{j-1} + \frac{M_2}{\alpha}\, b_o\,, \qquad j \geq 1\,.$$

Then for $j \geq 1$

$$\max\{\mathcal{U}_{2j}, \mathcal{U}_{2j+1}\} \;\leq\; \beta^j \max\{\mathcal{U}_0, \mathcal{U}_1\} \;+\; \frac{k M_1 M_2}{\alpha^2 (1-\beta)}\, b_o\,,$$

$$\max\{\mathcal{V}_{2j}, \mathcal{V}_{2j+1}\} \;\leq\; \beta^j \max\{\mathcal{V}_0, \mathcal{V}_1\} \;+\; \frac{M_2}{\alpha(1-\beta)}\, b_o\,.$$

Using the bounds on $\mathcal{U}_0$, $\mathcal{V}_0$ and (60) for $j = 0$, we get

$$\max\{\mathcal{U}_0, \mathcal{U}_1\} \leq \frac{b_o}{\alpha}\,, \qquad \max\{\mathcal{V}_0, \mathcal{V}_1\} \leq \left(\frac{M_1}{\alpha} + M_2 \right) \frac{b_o}{\alpha}\,. \quad (61)$$

Hence we obtain global bounds on U, V. Indeed,

$$\max_{\ell \geq 2} \mathcal{U}_\ell \;\leq\; \frac{b_o}{\alpha} \left\{ \beta + \frac{k M_1 M_2}{\alpha(1-\beta)} \right\} \doteq \tilde{\mathcal{U}}$$

$$\max_{\ell \geq 2} \mathcal{V}_\ell \;\leq\; \frac{b_o}{\alpha} \left\{ \beta \frac{M_1}{\alpha} + M_2 \left(\beta + \frac{1}{1-\beta} \right) \right\} \doteq \tilde{\mathcal{V}}\,.$$

Now we claim that, if b_o is sufficiently small, then (58), (59) are satisfied for all $j \geq 0$. First, we check for $j = 0, 1$, using (61). Then (58), (59) are satisfied respectively if

$$b_o B \frac{k M_1}{\alpha} \left[\frac{M_1}{\alpha} + M_2 \right] \leq 1 - \alpha\,, \qquad b_o B \left[\frac{M_1}{\alpha} + M_2 \right] \leq 1 - \alpha\,. \quad (62)$$

Since $kM_1 < \sqrt{k}M_1 < \alpha$, the second condition implies the first. For $j \geq 2$, (58) is satisfied if $\tilde{\mathcal{V}} k M_1 B \leq 1-\alpha$, that is

$$b_o B \left\{ \beta^2 + M_2 \frac{kM_1}{\alpha} \left(\beta + \frac{1}{1-\beta} \right) \right\} \;\leq\; b_o B \, \frac{1+2M_2}{\alpha(1-\beta)} \;\leq\; 1-\alpha \,, \tag{63}$$

while condition (59) is satisfied if $M_1 B \tilde{\mathcal{U}} \;+\; M_2 B b_o \leq 1-\alpha$, that is

$$b_o B \left\{ M_1 \frac{\beta}{\alpha} + \frac{M_2}{1-\beta} \right\} \;\leq\; b_o B \, \frac{M_1+M_2}{\alpha(1-\beta)} \;\leq\; 1-\alpha \,. \tag{64}$$

After some calculations, one verifies that the assumption (55) implies (62)–(64). □

Remark 5. The bound on the derivatives of the data, see (55), is proportional to $1/L$. We remark that (55) is a sufficient condition for the global existence and the proof is the same for both cases **(I)**, **(II)**, that is, it is treated in the same way the sign ± 1 in (45), (46) at $z = 0$. A more detailed analysis could be performed following the arguments presented in [3].

5. **Numerical results.** In this section we present a numerical validation of a model governed by the pressure relation (24) (here referred for simplicity as the "new model"), comparing it with the numerical results obtained by the model introduced in [23], in the inviscid case. We consider the case where all the parameters are constant.

For both models, we set $A(0,z) = A_0 > 0$, $Q(0,z) = 0$, $z \in [0,L]$. At the left boundary $z = 0$ we impose an area variation given by

$$A_{in}(t) = A_0(1 + 0.1 \sin(2\pi t/T_{per})), \quad t > 0$$

which guarantees that $\frac{A_{in}(t)}{A_0} \in [0.9, 1.1]$, $\forall\, t \geq 0$ and that $\left\| \frac{\partial A_{in}}{\partial t} \right\|_{C^0([0,+\infty))} \leq \frac{0.2 \cdot \pi \cdot A_0}{T_{per}}$. At the right boundary $z = L$ we are imposing $r = 0$. That is, we are considering boundary conditions in the form (41) with $\alpha = 1/2$ (i.e. $k = 0$). The data in the unit system CGS (centimeters, grams, seconds) are

$$L = 60\,,\; E = 4 \cdot 10^6\,,\; k_0 = 0.065\,,\; \xi = 0.5\,,\; A_0 = 1.76715\,,\; T_{per} = 0.8\,,\; \varrho = 1\,.$$

It may be verified that with this set of data inequality (48) is satisfied.

To discretize the two models we have adopted the second order Taylor-Galerkin scheme described in [13], which is a second-order accurate numerical scheme in the case of smooth solutions. The scheme has been implemented using the lifeV finite element library (www.lifev.org).

We consider a uniform mesh both in space and time with steps $\Delta z = 1$ and $\Delta t = 10^{-4}$, respectively. The numerical solution is smooth for both the cross-section area and the velocity (see Figures 4 and 5), for all simulation time. The simulation has been extended until the wave has completely left the domain.

A smooth solution has been obtained despite the fact that (55) is not satisfied, since in this case $b_o = 990.69$ while the right-hand side of (55) is equal to 126.55. This confirms that the inequality is only a sufficient condition. If we compare the characteristic speed for the new model and for the old model when $A = A_0$, we have

$$\textbf{char-speed-new} = \sqrt{\frac{\beta}{2}} \approx 461.17\,, \qquad \textbf{char-speed-old} = \sqrt{\frac{\beta_0}{2}} \approx 480.74\,,$$

which show that the two models are almost equivalent, with a slight slower propagation speed for the new one.

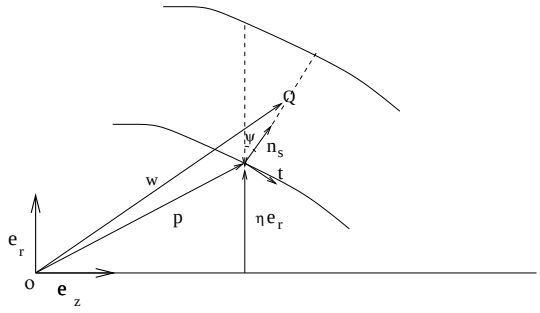

FIGURE 3. An axial section of the vessel at a given time t

We compare at $t = 0.1, 0.3, 0.5, 0.7$ the cross-section area in Figure 4 and the velocity in Figure 5 for both the new and the old model and remark that the numerical results are quite similar for the areas, while there are slight differences for the velocity. In fact, the two models have a different expression for the current characteristic speed (35). In the new model the coefficient $d = -\frac{1}{2} < 0$, causes a decrement of the characteristic speed with the increase of A, which is consistent with the elastic behavior. The old model has an opposite behavior, being $d = \frac{1}{2} > 0$. This could be more appropriate to simulate the stiffening characteristics of the wall of large arteries. In the following table we display the values of the C^0-norm of the ratio A/A_0 and of the velocity at the given times:

t	$\left\|\frac{A_{\text{new}}(t,\cdot)}{A_0}\right\|_{C^0([0,L])}$	$\|u_{\text{new}}(t,\cdot)\|_{C^0([0,L])}$	$\left\|\frac{A_{\text{old}}(t,\cdot)}{A_0}\right\|_{C^0([0,L])}$	$\|u_{\text{old}}(t,\cdot)\|_{C^0([0,L])}$
0.1	1.0344	15.51	1.0345	14.19
0.3	1.0477	21.68	1.0479	19.98
0.5	1.0112	17.01	1.0157	15.01
0.7	0.9635	24.67	0.9637	21.82

6. **Conclusions and further developments.** In this paper we have obtained a one-dimensional system describing the mean axial motion of a Newtonian incompressible fluid moving into a compliant straight vessel and the radial displacement of its isotropic and linearly elastic wall. The methodology can be extended to account for curvature and torsion. This extension is a subject of current research.

The analysis has demonstrated the well posedness of the problem under realistic data. This has been confirmed by numerical experiments.

Appendix A. **The metric of the wall.** In Figure 3 an axial section of the vessel at a given time $t \in [0, T]$ is presented.

Let us consider the vector-position of a point at the fluid-structure interface at a fixed time t given by:

$$p(t, \theta, z) = z\boldsymbol{e}_z + \eta(t, z)\boldsymbol{e}_r(\theta). \tag{65}$$

We recall that

$$\boldsymbol{e}_z = (0, 0, 1), \quad \boldsymbol{e}_r(\theta) = (\cos\theta, \sin\theta, 0), \quad \boldsymbol{e}_\theta(\theta) = \boldsymbol{e}_z \times \boldsymbol{e}_r = (-\sin\theta, \cos\theta, 0)$$

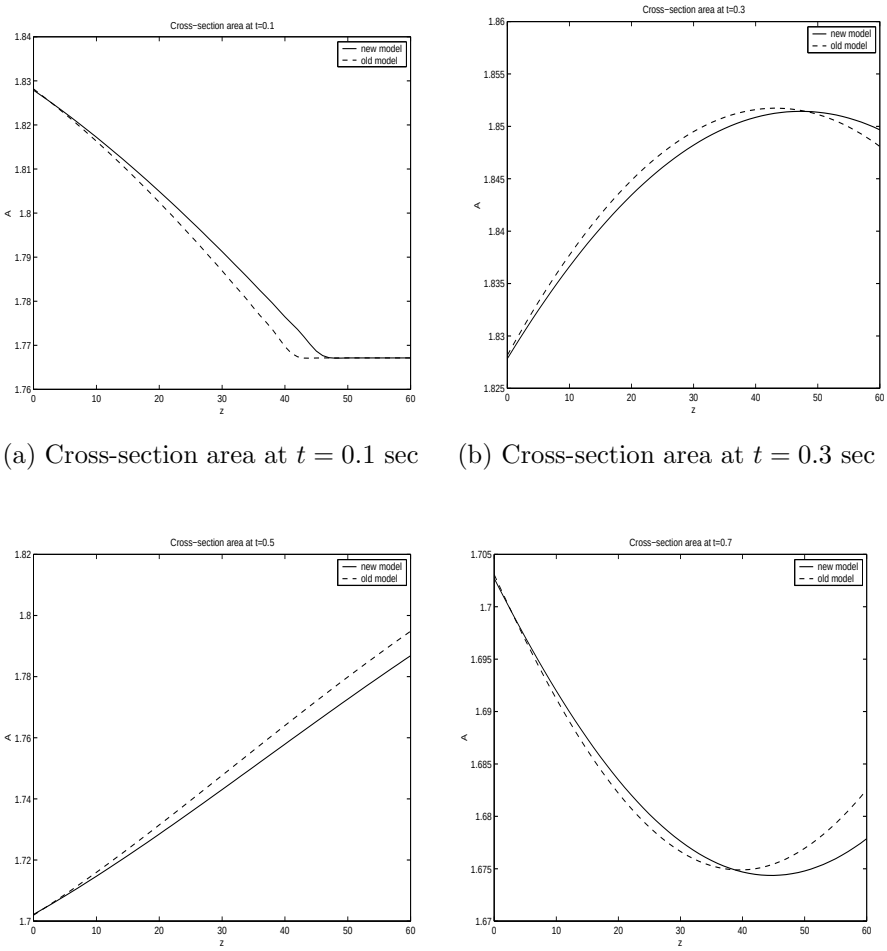

(a) Cross-section area at $t = 0.1$ sec (b) Cross-section area at $t = 0.3$ sec

(c) Cross-section area at $t = 0.5$ sec (d) Cross-section area at $t = 0.7$ sec

FIGURE 4. Cross-section area. Comparison between old model (dashed line) and new model (solid line).

where $\theta \in [0, 2\pi]$ is the phase angle around the vessel. We have that the local tangent to the fluid-structure interface profile is given by:

$$\boldsymbol{t}(t, \theta, z) = \left|\frac{\partial p}{\partial z}\right|^{-1} \left(\frac{\partial \boldsymbol{p}}{\partial z}\right) = \left[1 + \left(\frac{\partial \eta}{\partial z}\right)^2\right]^{-1/2} \left(\boldsymbol{e}_z + \frac{\partial \eta}{\partial z}\boldsymbol{e}_r(\theta)\right).$$

This relation is consistent with the expression of the local outward normal to the fluid-structure interface, given in (2) by:

$$\boldsymbol{n}_s(t, \theta, z) = \left[1 + \left(\frac{\partial \eta}{\partial z}\right)^2\right]^{-1/2} \left(-\frac{\partial \eta}{\partial z}\boldsymbol{e}_z + \boldsymbol{e}_r(\theta)\right).$$

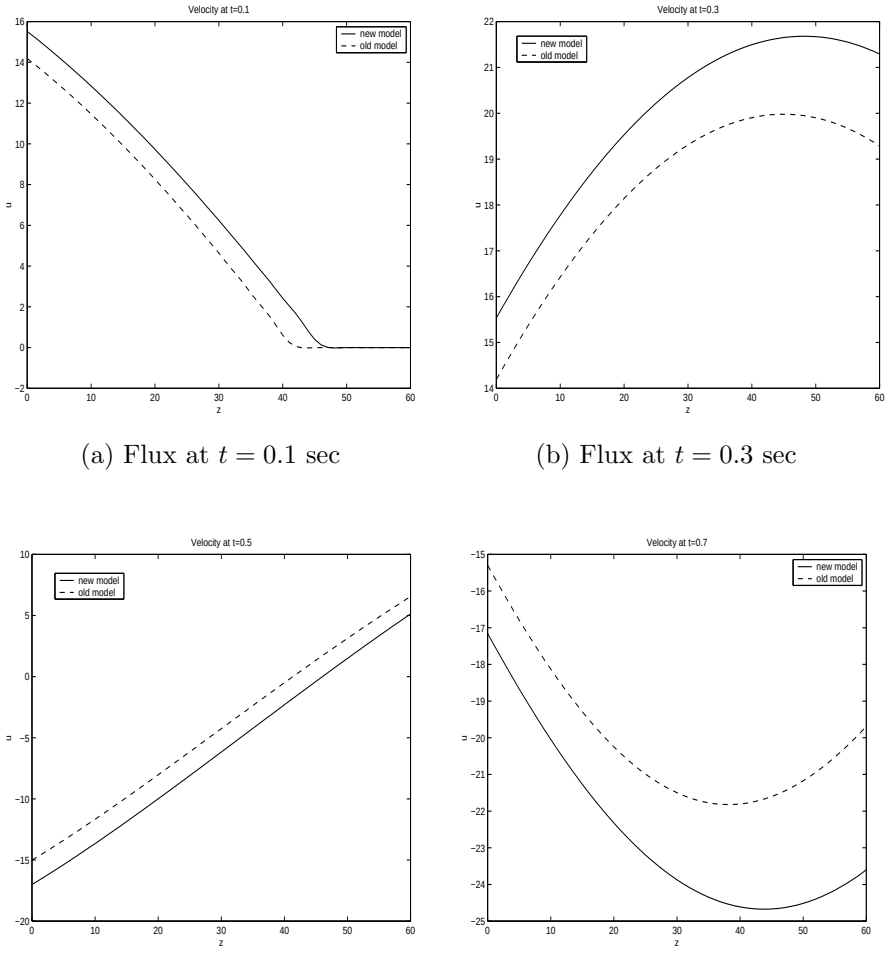

(a) Flux at $t = 0.1$ sec

(b) Flux at $t = 0.3$ sec

(c) Flux at $t = 0.5$ sec

(d) Flux at $t = 0.7$ sec

FIGURE 5. Velocity. Comparison between old model (dashed line) and new model (solid line).

Let us consider on the vessel wall the three independent variables s, θ, l: $\theta \in [0, 2\pi]$ is the usual circumferential variable, l is the arc-length on the vessel wall profile, given by:

$$l(z) = \int_0^z \left[1 + \left(\frac{\partial \eta}{\partial z}\right)^2\right]^{1/2} dz\,, \qquad z \in [0, L]$$

while $s \in [0, k(t, z)]$ is the position along the local normal $\boldsymbol{n}_s$ to the vessel wall surface. Here $k = k(t, z)$ is the thickness of the vessel wall. The position of a general point Q in the wall is given by (see Figure 3):

$$\boldsymbol{w}(s, \theta, l) = Q - 0 = z\boldsymbol{e}_z + \eta \boldsymbol{e}_r(\theta) + s\boldsymbol{n}_s(t, \theta, z) \tag{66}$$

The derivatives of the position vector (66) with respect to the local variables s, θ, l are given at time t by:

$$a_1 = \frac{\partial \boldsymbol{w}}{\partial s} = \boldsymbol{n}_s(t,\theta,z)$$
$$a_2 = \frac{\partial \boldsymbol{w}}{\partial \theta} = (\eta + s\cos\psi)\boldsymbol{e}_\theta(\theta)$$
$$a_3 = \frac{\partial \boldsymbol{w}}{\partial l} = \boldsymbol{t}(t,\theta,z) = (1+s\chi(t,z))\boldsymbol{t}(t,\theta,z)$$

where we posed:

$$\cos\psi = \left[1+\left(\frac{\partial\eta}{\partial z}\right)^2\right]^{-1/2}, \qquad \chi(t,z) = -\frac{\partial^2\eta}{\partial z^2}\left[1+\left(\frac{\partial\eta}{\partial z}\right)^2\right]^{-3/2}. \tag{67}$$

Remark that $\chi(t,z)$ is the curvature of the line described by the point p introduced in (65) as z varies at fixed t while the quantity $\eta + s\cos\psi$ represents the radial distance of the point Q determined by the vector position (66) from the centerline of the vessel.

The metric induced by $\boldsymbol{w}$ is orthogonal and given in covariant form by:

$$\underline{G} = g_{ij} = a_i \cdot a_{j\,i,j\in\{1,2,3\}} = \begin{bmatrix} h_s^2 & 0 & 0 \\ 0 & h_\theta^2 & 0 \\ 0 & 0 & h_l^2 \end{bmatrix} \tag{68}$$

where:

$$h_s = 1, \quad h_\theta = r = \eta + s\cos\psi, \quad h_l = 1 + s\chi(t,z)\,. \tag{69}$$

Acknowledgments. The first author acknowledges support by *Progetto GNAMPA 2005*, titled *Analisi Asintotica Per Sistemi Iperbolici Nonlineari*. The second author acknowledges the support of the Politecnico di Milano through the "CIRIC" grant. The third author wishes to thank the European Commission and the Italian MIUR for financial support, respectively through the RTN project HaeMOdel and the project "COFIN 2005".

Finally, the authors wish to thank Prof. D. Serre for pointing out reference [3] and Prof. A. Veneziani for his interest and suggestions.

REFERENCES

[1] S. Alinhac, "Blowup for Nonlinear Hyperbolic Equations," Birkhäuser, Boston, 1995.
[2] R. Aris, "Vectors, Tensors and The Basic Equations of Fluid Mechanics," Prentice-Hall, 1962.
[3] P. Bergeret, *Classification of smooth solutions to* 2×2 *hyperbolic systems with boundary damping*, Math. Meth. Appl. Sci., **20** (1997), 1563–1598.
[4] S. Čanić, E. H. Kim, *Mathematical analysis of the quasilinear effects in a hyperbolic model blood flow through compliant axi-symmetric vessels*, Math.Meth.Appl.Sci., **26** (2003), 1161–1186.
[5] S. Čanić, D. Lamponi, A. Mikelić, J. Tambaća, *Self-consistent effective equations modelling blood flow in medium-to large compliant arteries*, Multiscale Model. Simul., **3** (2005), 559–596.
[6] C. M. Dafermos, "Hyperbolic Conservation Laws in Continuum Physics" (1^{st} Ed.), Springer Verlag, Berlin, 2000.
[7] A. Di Carlo, P. Nardinocchi, G. Pontrelli, L. Teresi, *A heterogeneous approach for modelling blood flow in an arterial segment*, in "Simulation in Biomedicine V" (eds. Z. M. Arnez, C.A. Brebbia, F. Solina & V. Stankovski), WIT Press, 2003, 69–78.
[8] S. Ferrari, F. Saleri, *A new two-dimensional shallow water model including pressure effects and slow varying bottom topography*, ESAIM: M2AN, **38** (2004), 211–234.

[9] S. Ferrari, *Convergence analysis of a space-time approximation to a two-dimensional system of shallow water equations*, Applicable Analysis, **83** (2004), 757–785.
[10] L. Formaggia, J.-F. Gerbeau, F. Nobile, A. Quarteroni, *On the coupling of 3D and 1D Navier-Stokes equations for flow problems in compliant vessels*, Comp.Methods in Appl.Mech.Engng.,**191** (2001), 561–582.
[11] L. Formaggia, D. Lamponi, A. Veneziani, M. Tuveri, *Numerical modeling of 1D arterial networks coupled with a lumped parameters description of the heart*, Computer Methods in Biomechanics and Biomedical Engineering, 2007, (to appear).
[12] L. Formaggia, F. Nobile, A. Quarteroni, A. Veneziani, *Multiscale modelling of the circulatory system: a preliminary analysis*, Comp. Vis. Science, **2** (2000), 163–197.
[13] L. Formaggia, A. Veneziani, *Geometrical multiscale models for the cardiovascular system*, in "Blood Flow Modelling and Diagnostics" (ed. T.A. Kowaleski), Institute of Fundamental Technological Research, Warsaw, (2005), 309–360.
[14] Y. C. Fung, "Foundations of Solid Mechanics," Prentice-Hall, Englewood Cliffs N.J, 1972.
[15] Y. C. Fung, K. Fronek, P. Patitucci, *Pseudoelasticity of arteries and the choice of its mathematical expression*, Amer. Physiology Soc., (1979), 620–631.
[16] J.-F. Gerbeau, B. Perthame, *Derivation of viscous Saint-Venant system for laminar shallow water; numerical validation*, Discrete Contin. Dyn. Syst. Ser. B, **1** (2001), 89–102.
[17] J. M. Greenberg and T.-T. Li, *The effect of boundary damping for the quasilinear wave equation*, J. Differential Equations, **52** (1984), 66–75.
[18] L. Hörmander, "Lectures on Nonlinear Hyperbolic Differential Equations," Springer-Verlag, New York, 1997.
[19] D. Lamponi, *One dimensional and multiscale models for blood flow circulation*, Phd Thesis n. 3006, EPFL, Lausanne, (2004).
[20] T.-T. Li, "Global Classical Solutions for Quasilinear Hyperbolic Systems," Masson, Paris, 1994.
[21] A. Majda, "Compressible Fluid Flow and Systems of Conservation Laws in Several Space Variables," Springer-Verlag, New York, 1984.
[22] T. Pedley, "The Fluid Mechanics of Large Blood Vessels," Cambridge University Press, Cambridge, 1980.
[23] A. Quarteroni and L. Formaggia, *Mathematical modelling and numerical simulation of the cardiovascular system*, in "Handbook of Numerical Analysis" (Vol. XII) , North Holland, Amsterdam, 2004, 3–127.
[24] S. J. Sherwin, V. Franke, J. Peiró and K. Parker, *One dimensional modelling of a vascular network in space-time variables*, J.Eng.Math., **47** (2003), 217–250.
[25] N. P. Smith, A. J. Pullan and P. J. Hunter, *An anatomically based model of transient coronary blood flow in the heart*, SIAM J. Appl. Math., **62** (2002), 990–1018.

Received July 2006; revised December 2006.

E-mail address: amadori@univaq.it
E-mail address: steferrarigia@tiscalinet.it
E-mail address: luca.formaggia@polimi.it